4th International Conference on Gas Hydrates

May 19-23, 2002, Yokohama

Hydrate Formation Rate in a Continuous Stirred Tank Reactor: Experimental Results and Bubble-to-Crystal Model

Marit Mork* and Jon S. Gudmundsson

Department of Petroleum Engineering and Applied Geophysics, Norwegian University of Science and Technology, 7491 Trondheim, Norway

The rate of hydrate formation is an important parameter in the production of hydrates for transport and storage of natural gas and in cold flow technology. In a continuous stirred tank reactor of 9 liter, methane and natural gas hydrate formation rates have been measured at steady-state conditions at 70 to 90 bar and 7 to 15 °C. Experimental results show that the formation rate is controlled mainly by the gas injection rate into the reactor and the pressure. The effect of the temperature driving force is negligible. At similar conditions, no difference has been observed between methane and natural gas hydrate formation rates. The rate of hydrate formation is found to be dominated by transport processes rather than growth kinetics. A bubble-to-crystal model has been developed for the transport of gas from a gas bubble to a hydrate crystal surface. The model predicts the rate of hydrate formation in a continuous stirred tank reactor satisfactorily.

Introduction

The rate of hydrate formation is identified as one of the critical parameters in design and operation of large-scale hydrate production plants for storage and transport of gas as hydrates. At the Norwegian University of Science and Technology (NTNU), extensive studies of relevant hydrate properties have been carried out (Gudmundsson *et al.*, 2002). In the production process, hydrates are formed in a continuous water phase at typically 5-15 °C and 50-100 bar. The same conditions are relevant in cold flow technology where oil, gas and water are passed through a subsea unit for flow assurance purposes (Gudmundsson, 2002).

In this study, the rate of hydrate formation has been measured in a continuous stirred tank reactor (CSTR) under various pressure, temperature and hydrodynamic conditions. To describe the rate of hydrate formation in a CSTR, a bubble-to-crystal model has been developed.

Hydrate Formation Studies

The hydrate formation process has been identified by many researchers as important in understanding the nature of gas hydrates. Vysniauskas and Bishnoi (1983, 1985) initiated a systematic research on hydrate formation kinetics by studying the rate of methane and ethane hydrate formation in a semi-batch stirred reactor. They proposed a semi-empirical model, with pressure, gas-liquid interfacial area and temperature driving force, for the rate of gas consumption, and a mechanism for nucleation and growth.

Englezos *et al.* (1987) studied the formation of methane and ethane hydrates, and proposed a model where the rate of gas consumption was coupled to the crystal growth rate using both crystallization theory, including the particle size distribution, and mass transport two-film theory. Other hydrate formation models for semi-batch reactors, including mass transport, growth and other crystallization phenomena, have been proposed by Herri *et al.* (1999) and Monfort *et al.* (2000). Herri *et al.* pointed out the crucial importance of gas-liquid mass transfer. Bollavaram *et al.* (2000) studied the growth rate of tetrahydrofuran hydrates by eliminating successfully the mass transfer effects and partly the heat transfer effects on hydrate formation. They found that the growth rate increased with temperature driving force.

Skovborg and Rasmussen (1994) discussed the model of Englezos *et al.* and concluded that the hydrate formation rate was mass transport limited and thus independent of the total particle surface area. Then, the need for information about the particle size distribution was eliminated. Skovborg and Rasmussen proposed a model where transport of gas to the liquid water phase is the rate-determining step in hydrate formation.

Happel *et al.* (1994) studied the formation rate of methane and methane-nitrogen hydrates in a CSTR of 1 liter. The measured formation rates were found to be much higher than those of Vysniauskas and Bishnoi (1983), which led to the conclusion that applying results from semi-batch reactors could prove difficult in design of a continuous hydrate formation reactor.

Experiments

Experiments were performed in the Natural Gas Hydrate laboratory at NTNU, a laboratory designed to study the formation of hydrates and their properties.

Laboratory. A schematic drawing of the laboratory is shown in Figure 1. The laboratory has a flow loop consisting of four main units: a CSTR, a separator, a shell-and-tube heat exchanger and a centrifugal slurry pump. The CSTR is a 9-liter reactor of standard design with four baffles and a Rushton impeller with 6 blades.

*Corresponding author. E-mail: mmork@ipt.ntnu.no

Maximum rotational speed of impeller is 2500 RPM. Natural gas mixture or methane gas is injected from gas bottles into the reactor through two non-return valves located at the bottom of the reactor. Gas and hydrate slurry are taken out at the top and the bottom of the separator, respectively. The heat exchanger removes heat from hydrate formation and heat added from various equipment

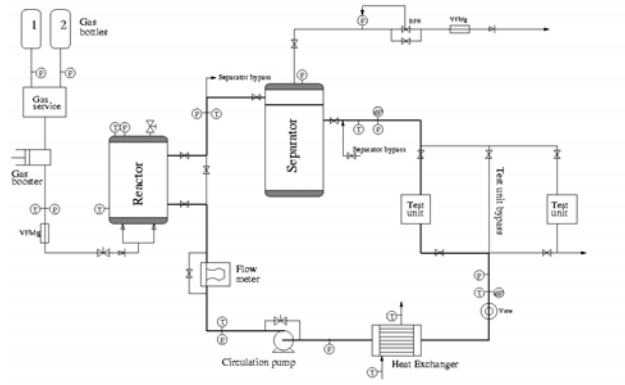

Figure 1 Schematic drawing of Natural Gas Hydrate laboratory.

components. The slurry pump circulates the fluid in the loop.

The loop is designed to operate at pressures up to 120 bar, and temperatures in the range 0-20 °C. It is Ex-II classified and situated in a temperature-controlled room. A data acquisition system records gas flow rates and temperature and pressure at various locations in the rig. A backpressure regulator on the gas exit line enables constant pressure during experiments.

Method. In the present study, the rate of methane and natural gas hydrate formation was measured at steady-state conditions. The natural gas mixture consisted of 92 % methane, 5 % ethane and 3 % propane (mole %). To minimize fractionation when producing natural gas hydrates, the experimental pressure and temperature were chosen so that hydrates were formed far into the hydrate region (Levik *et al.*, 2002). The experimental pressure was 70 or 90 bar absolute pressure. The experimental temperature was 7 °C in methane experiments and 12.5 to 15 °C in natural gas experiments. The stirring rate was 400 RPM. Steady-state hydrate formation was accomplished by keeping gas injection rate, stirring and circulation of the fluid constant during the experiment.

At start of the experiment, the flow loop was filled with de-aerated tap water. The separator was left half-full with a gas pocket to avoid water in the gas exit line. The loop was pressurized with methane or natural gas mixture to about 5 bar below the hydrate equilibrium pressure at the experimental temperature and left overnight for gas dissolution. The next day, the loop was pressurized to the experimental pressure and data acquisition started.

Stirring, circulation and gas injection were started simultaneously, and hydrate formation commenced almost immediately. The gas vent rate was measured with a flow meter. Constant gas injection rate was maintained by providing constant inlet pressure. The rate was calculated, in terms of Nl/min where normal conditions are 1 atmosphere and 0 °C, using real gas law for the gas bottle volume. After some minutes, when stable flow was obtained, gas injection rate was changed or experiment stopped. Gas consumption rate was calculated from the difference in gas injection and gas vent rates.

Hydrate Formation Results

The rate of hydrate formation has been measured under different conditions by varying pressure, temperature, gas injection rate and gas composition. Also, a single experiment with methane gas at a stirring rate of 800 RPM has been performed. Similarly, two experiments with natural gas mixture at high subcooling, were performed. The main objective, however, was to investigate the effect of high gas injection rates to resemble conditions in industrial gas-liquid dispersion reactors. The result of a typical experiment is shown in Figure 2.

The results of methane gas experiments at 70 and 90 bar at 7 °C are shown in Figure 3. Gas consumption rate appears to be proportional to the gas injection rate. The dashed lines are the linear trend lines for each isobar, indicating that formation rate increases with increased pressure. It should be noted that while the line for 70 bar results intersects close to origo, the line for 90 bar results does not. Previous results of Parlaktuna and Gudmundsson (1998a, 1998b) show that at 90 bar at low gas injection rates, a linear trend line intersects close to origo. Plotting both present and previous results for 90 bar, a linear trend line intersecting near origo is obtained.

A single experiment carried out with variation in stirring rate at high gas injection rate at 70 bar and 7 °C, shows that from 400 RPM to 800 RPM the gas consumption rate increases from 79.0±10.6 Nl/min to 88.7±10.1 Nl/min. The increase in hydrate formation rate when doubling the stirring rate, is small relative to the effect of gas injection rate.

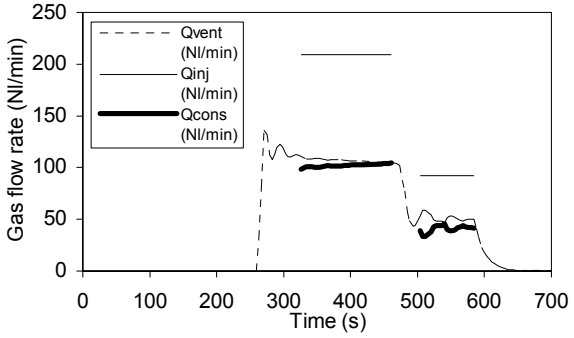

Figure 2 Experiment 3a at 70 bar and 7.2 °C. Methane gas. The gas injection rate was changed after about 460 seconds.

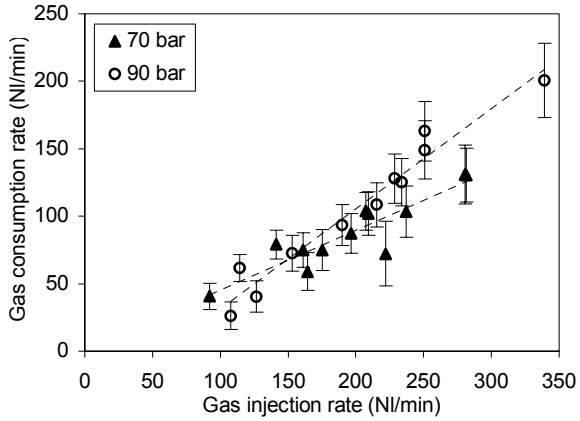

Figure 3 Methane gas consumption rate as a function of gas injection rate at 70 and 90 bar at 7 °C.

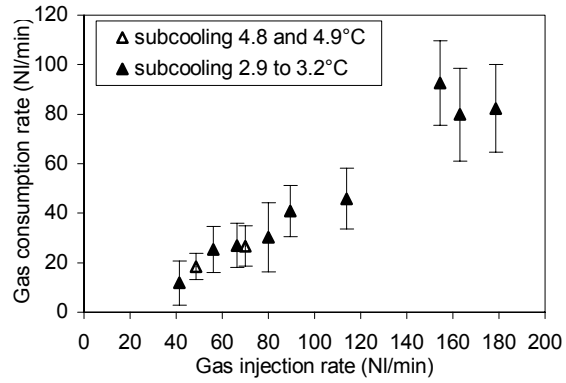

Figure 4 Natural gas mixture consumption rate as a function of gas injection rate rate at 70 bar and approximately 3 °C subcooling.

Results from 70 bar experiments with natural gas mixture are shown in Figure 4. As observed for methane hydrate formation, gas consumption rate is proportional to the gas injection rate. Also, two experiments were performed at 4.8 and 4.9 °C subcooling. No effect of increasing the subcooling from about 3 °C to 5 °C is observed.

Methane gas and natural gas mixture results are compared in Figure 5. Subcooling was approximately 3 °C in both groups of experiments. It should be noted, however, that the absolute temperature in methane and natural gas mixture experiments was about 7 and 15 °C, respectively. The fundamental difference between structure I and structure II hydrates appears not to affect the hydrate formation rate under the present conditions.

The maximum error in each gas consumption rate is indicated with error bars in the figures, being approximately 15% and 30% of the calculated rate itself for methane gas and natural gas mixture, respectively. The error estimation is conservative. Also, the relative large inaccuracy can be explained by the method of measuring the gas injection rate and by the difficulty of performing the experiments. The gas volume injected was found from real gas law and averaged over the time period, giving the gas injection rate. Therefore, errors in pressure, temperature and volume measurements, and error in calculated z-factor, are included in the overall error in gas injection rate. In performing an experiment, stabilizing the gas injection and gas vent rates for a sufficiently long time was challenging. The period of time where gas injection and gas vent rates were averaged, also affected the overall error in gas consumption rate.

Investigated Parameters

The experimental results show that the gas injection rate and pressure are the most important parameters investigated. Gas injection rate is one of the parameters affecting the gas-liquid interfacial area, which is identified by many researchers as an important parameter in hydrate formation (Englezos *et al.*, 1987, Monfort *et al.*, 2000). By increasing gas injection rate, more bubbles are formed, increasing the gas-liquid interfacial area.

Gas liquid interfacial area is also affected by stirring. In present experiments, a small effect of stirring is

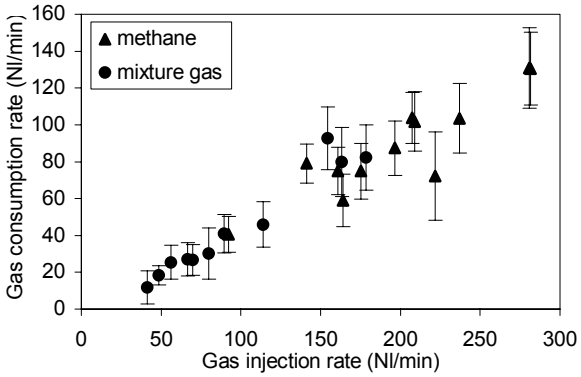

Figure 5 Gas consumption rate as a function of gas injection rate for methane gas and natural gas mixture. Pressure is 70 bar, and subcooling is approximately 3 °C in experiments with both gas compositions.

observed. Previous results (Parlaktuna and Gudmundsson, 1998a, 1998b) demonstrate that the formation rate increases faster at low stirring rates than at high stirring rates. In a CSTR, complete dispersion of the gas phase occurs when stirring rate is sufficiently high to disperse all the gas entering the reactor. When there is a shortage of gas, bubbles are recirculated in the reactor (Tatterson, 1991). Thus, the minor effect of stirring observed can be explained by a complete dispersion or recirculation of the gas in the reactor. This conclusion is supported by the fact that compared to industrial gas-liquid dispersion processes, the superficial gas velocity in present experiments was about two orders of magnitude smaller. Superficial gas velocity is the volumetric flow rate of gas per cross sectional area of reactor. The gas injection rate (the superficial gas velocity) was limited by the size of the laboratory gas injection system.

The results show an effect of pressure on the gas consumption rate. The effect of pressure may have two possible explanations. First, increased pressure results in larger driving force for hydrate formation, the difference between experimental pressure and hydrate equilibrium

pressure at the same temperature. Others (Monfort *et al.*, 2000, Vysniauskas and Bishnoi, 1983) have observed that the rate of hydrate formation increases with increased driving force. Second, at 90 bar the solubility of hydrocarbon gases in water is higher than at 70 bar. With increased solubility in the water phase, more gas is available for nucleation and growth.

No significant effect of subcooling is observed in either present or previous results (Parlaktuna and Gudmundssson, 1998a, 1998b), which implies that the temperature driving force is not controlling the rate of hydrate formation. In addition, no difference in rate, at equal subcooling, but different temperature, is observed between the rate of methane gas and natural gas hydrate formation. Therefore, it is believed that transport processes rather than kinetic processes dominate hydrate formation. The effect of pressure driving force can be ascribed to the increased solubility, as discussed above. That transport processes, primarily mass transport, control hydrate formation is supported by the findings of Skovborg and Rasmussen (1994).

Hydrate Formation Model

Hydrate formation can be considered as a transport process where the combined heat and mass transfer effects are important. The experimental results indicate that hydrate formation is a combined diffusion and reaction process where diffusion is dominating. Based on this observation, the bubble-to-crystal model is proposed, and mass transfer is chosen to represent the transport processes in the system. The hydrate forming system consists of bubbles and growing hydrate particles dispersed in a continuous water phase, as illustrated in Figure 6. Gas is transported between the three phases. Driving forces are written in terms of concentration differences.

The bubble-to-crystal model is based on three steps. First, gas is transported by molecular diffusion from the gas-water interface to the liquid bulk phase through a liquid film. At the interface, gas and liquid phases are in equilibrium. Temperature increases due to enthalpy of solution. Second, gas is transported due to molecular and eddy diffusion through the liquid bulk phase, which has a uniform gas concentration and temperature, to the liquid film surrounding the hydrate crystal. Third, gas diffuses through the liquid film to the hydrate crystal surface and is incorporated into the hydrate structure. Temperature increases due to enthalpy of hydrate formation.

Assuming no accumulation in the liquid film surrounding the gas bubble and using simple film theory, the following equation for the rate of gas dissolution is suggested:

$$r_1 = k_L A_g (C_{sol} - C_b) \qquad (1)$$

where k_L is the gas-liquid mass transfer coefficient, A_g is the interfacial area, C_{sol} is the gas concentration at the gas-liquid interface and C_b is the concentration of gas in the liquid bulk phase. The gas concentration at the interface is given by the mole fraction solubility of gas in water at the experimental conditions:

$$C_{sol} = \frac{x(P,T)\,\rho_{H_2O}}{M_{H_2O}}$$

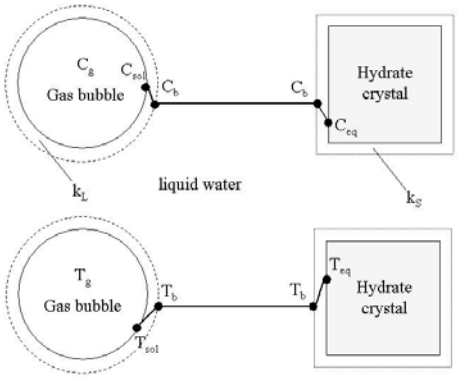

Figure 6 Schematic drawing of the bubble-to-crystal model illustrating the concentration and temperature differences as gas is transported from gas bubble to hydrate crystal.

The next concentration drop is from liquid bulk to hydrate crystal surface. According to standard diffusion theory (Mullin, 1993), for each consecutive step in the transport of solute to crystal surface, rate equations can be established. Again, assuming no accumulation in the film, a proportional concentration driving force for the gas consumption rate can be expressed by:

$$r_2 = k_S A_c (C_b - C_{eq}) \qquad (2)$$

where k_S is a rate constant for the diffusion through the liquid film surrounding the crystal and A_c is the liquid-crystal interface area. C_{eq} is the gas concentration at the crystal surface where gas and water are in equilibrium with hydrate. The temperature is equal to the hydrate equilibrium temperature. The concentration at the hydrate surface is the solubility of gas in water at experimental pressure and equilibrium (not experimental) temperature:

$$C_{eq} = \frac{x(P,T_{eq})\,\rho_{H_2O}}{M_{H_2O}}$$

Assuming that hydrate formation is controlled by diffusion through the interfaces and not by growth, the overall rate of hydrate formation can be written as:

$$r = K(C_{sol} - C_{eq}) \qquad (3)$$

where

$$\frac{1}{K} = \frac{1}{k_L A_g} + \frac{1}{k_S A_c} \qquad (4)$$

Equation (3) applies to the total gas consumption rate for the whole reactor if it is multiplied with the liquid volume of the reactor.

Similar to the approach of Skovborg and Rasmussen (1994), the model can be extended to more than one hydrate-forming component by assuming that the transport rates are independent of each other:

$$r_{tot} = \sum_{i=1}^{n} K_i (C_{sol,i} - C_{eq,i}) x_i \qquad (5)$$

where n is the total number of gas components and x_i is the mole fraction of the component in the gas phase.

Parameter Estimation

For the present experiments, the bubble-to-crystal model can be applied by assuming perfect mixing so that no concentration or temperature gradients occur in the bulk volume. Also, the hydrate crystals and gas bubbles are assumed to be uniformly distributed. Since experiments were performed at constant gas injection rate, stirring rate, pressure and temperature, steady-state conditions can be assumed, which imply that the concentration driving force is constant throughout an experiment for a given set of experimental conditions. Since gas consumption rate remained constant during an experiment, hydrate formation rate was not affected by the amount of hydrate crystals present in the reactor, even though the hydrate slurry was recirculated to the reactor. The model is based on gas concentrations. Water is in excess and is assumed not to limit the rate of hydrate formation.

Solubility is an important parameter in the bubble-to-crystal model, determining the gas concentration at both the gas-liquid interface and at the crystal surface. Data on methane, ethane and propane solubility at high pressure and low temperature is limited. Due to lack of data at the present conditions, Henry's law solubility data (Perry and Green, 1984, Kobayashi and Katz, 1951) was used in the calculation of gas concentrations. Moreover, the solubility of methane calculated from Henry's law, was found to be higher and closer to the solubilities found by Song *et al.* (1997) and Besnard *et al.* (1997), than the solubility calculated using Battino's correlation (Battino and Clever, 1966). Song *et al.* and Besnard *et al.* investigated the solubility of methane near hydrate forming conditions and found it to be much higher than what is reported by others, however, too few data was presented to be useful in this study.

To estimate the combined mass transfer coefficient in Equation (4), a customary correlation to determine the gas-liquid mass transfer coefficient in stirred tank reactors of standard design, was adopted. In this study, the correlation was assumed to be adequate for mass transfer through the gas-liquid interface and through the liquid-crystal interface. Thus, the overall mass transfer coefficient was represented by a relationship containing the power consumption and the superficial gas velocity (Tatterson, 1991):

$$K = \alpha \left(\frac{P_g}{V} \right)^{\beta} (v_{sg})^{\gamma} \qquad (6)$$

where V is the reactor volume, v_{sg} is the superficial gas velocity and P_g is the gassed power consumption given by:

$$P_g = (1 - 12.6 Fl_g) P_u \qquad (7)$$

valid only for gas flow numbers $Fl_g = Q_g/ND^3$ less than 0.035 (valid for present conditions). Ungassed power consumption is given by (Oldshue, 1983):

$$P_u = N_p \rho N^3 D^5 \qquad (8)$$

For Rushton impellers, power number N_p is 5 (Tatterson, 1991). Density ρ was taken as the density of water. Impeller diameter D was 760 mm, and stirring rate N was 400 RPM. Equation (6) is empirical in nature, and α, β and γ depend on reactor geometry and fluids. The overall rate of methane hydrate formation for the total liquid volume was modeled using:

$$R = \alpha \left(\frac{P_g}{V} \right)^{\beta} (v_{sg})^{\gamma} (C_{sol} - C_{eq}) V \qquad (9)$$

where V is the liquid volume where hydrate formation occurs.

The fitting parameters, α, β and γ, were found by minimizing the sum of squares of the differences between experimental and calculated gas consumption rates using Equation (9). The regression was performed using a commercially available computer program featuring multiple non-linear regression (Polymath 5.1, 2002). For natural gas mixture, the overall mass transfer coefficients were assumed equal for all components. Calculated regression parameters and their 95% confidence intervals for methane are shown in Table 1. The regression is based on results from both present and previous experiments (Parlaktuna and Gudmundsson, 1998a, 1998b).

Table 1 Calculated values of parameters in Equation (9) for methane gas experiments.

	Liquid volume $9 \cdot 10^{-3}$ m^3		Liquid volume $34 \cdot 10^{-3}$ m^3	
	Mean value	95% confidence limit	Mean value	95% confidence limit
α	278.7	286.4	97.06	88.96
β	0.2065	0.1517	0.2065	0.1517
γ	1.144	0.129	1.144	0.129

Table 2 Calculated values of parameters in modified Equation (5) for natural gas mixture experiments.

	Liquid volume $9 \cdot 10^{-3}$ m^3	
	Mean value	95% confidence limit
α	72.94	245.5
β	0.9197	0.6797
γ	1.501	0.2137

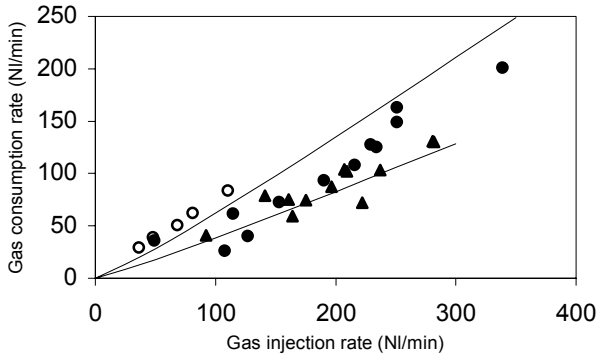

Figure 7 Comparison of bubble-to-crystal model with

experimental data for methane gas at 7 °C and 400 RPM. Lower line represent 70 bar, upper line 90 bar. Triangles are experimental data at 70 bar, bullets at 90 bar. Circles are previous experiments at 90 bar (Parlaktuna and Gudmundsson, 1998a, 1998b).

The formation rate was modeled by using both the liquid volume of the CSTR ($9 \cdot 10^{-3}$ m^3) and the total liquid volume of the rig ($34 \cdot 10^{-3}$ m^3), as shown in Table 1. Calculated regression parameters for natural gas mixture, also including both present and previous results, are shown in Table 2.

Discussion

The model was fitted with experimental data to determine the exponents in Equation (9). The mean values and their 95% confidence intervals are shown in Table 1 and Table 2 for methane gas and natural gas mixture, respectively. Using the volume of the whole rig (34 liter) instead of the volume of the CSTR (9 liter) in Equation (9), the 95% confidence limit of α becomes lower than the mean value of α. This improvement indicates that when the liquid volume where hydrates form is increased, a better fit of the data is obtained. In practice, hydrate formation is probably not restricted to the CSTR, but may also take place in the flow loop, despite of gas separation downstream the reactor. The circulation pump provides turbulent mixing in the flow loop.

The value of exponent γ, demonstrates that the gas hydrate formation rate is almost proportional to the superficial gas velocity, as shown in Figure 3, Figure 4 and Figure 5. Similarly, the value of exponent β in Table 1 proves that the dependence of stirring rate is weak. Confidence limits are smaller than the mean values, and the mean values are therefore believed to be reliable.

For natural gas mixture (Table 2), the confidence limit of parameter α is higher than the mean value. Increasing the liquid volume, as done for methane, did not lower the confidence limit. The accuracy is poorer than for methane gas because the experimental data points were fewer and had larger errors due to more complications in the natural gas mixture experiments. For the most part, the experimental inaccuracy is included in α.

In Figure 7, the bubble-to-crystal model is applied to predict the methane hydrate formation rate at 70 and 90 bar using the parameters for 34 liter liquid volume in Table 1. At 70 bar, the prediction corresponds well with the experimental results. At 90 bar, the bubble-to-crystal model overestimates the formation rate for present results and underestimates for previous results (Parlaktuna and Gudmundsson, 1998a, 1998b). The reason could be the quality of the experimental data at 90 bar. As shown in Figure 3, the data deviates from the linear trend assumed for gas injection rate versus gas consumption rate.

The bubble-to-crystal model describes the transport of gas from gas bubble to crystal surface and assumes that the diffusion of gas from bubble to liquid bulk and from liquid bulk to crystal surface are the rate-determining steps. This makes the model a useful engineering model where the necessary parameters can be measured directly, calculated or found by regression. Others (Englezos *et al.*, 1987, Herri *et al.*, 1999) have included the particle size distribution, but considering the difficulty of particle size measurements and the quality of such results, the bubble-to-crystal model seems to give a sufficiently good prediction of the hydrate formation rate in a continuous stirred tank reactor.

The simplicity of the bubble-to-crystal model was facilitated by the use of a CSTR that operates at steady-state conditions, which is relevant in design and operation of large-scale reactors for hydrate production.

Conclusions

The rates of methane and natural gas hydrate formation have been measured at conditions relevant for production of natural gas hydrates in continuous stirred tank reactors. The rate of formation was found to be most dependent of the gas injection rate into the reactor and pressure, and less dependent of stirring. The effects of temperature driving force and gas composition, forming both structure I and II hydrates, were negligible. The experimental results indicated that heat and mass transport processes dominated the formation process. A bubble-to-crystal model was chosen for the rate of hydrate formation in a continuous stirred tank reactor. The proposed model was found to describe the experimental data satisfactorily.

Acknowledgments

The Research Council of Norway is thanked for supporting the doctoral work of Marit Mork through the NATURGASS program contract no. 125482/212.

References

Battino, R. and Clever, H.L. (1966). The Solubility of Gases in Liquids, *Chem. Rew.*, **66**, 4, 395-463.

Besnard, G., Song, K.Y., Hightower, J.W., Kobayashi, R., Elliot, D. and Chen, R. (1997). New Method of Temperature-Ramping, Isobaric Experiments to Study the Hydrate Formation and Decomposition, *American Chemical Society*, **42**, 2.

Bollavaram, P., Devarakonda, S., Selim, M.S. and Sloan, E.D. (2000). Growth Kinetics of Single Crystal sII Hydrates, Elimination of Mass and Heat Transfer Effects, *Annals of New York Academy of Sciences,* **912**, 533-543.

Englezos, P., Kalogerakis, N., Dholabhai, P.D. and Bishnoi, P.R. (1987). Kinetics of Formation of Methane and Ethane Gas Hydrates, *Chemical Engineering Science*, **42**, 11, 2647-2658.

Gudmundsson, J.S., Mork, M. and Graff, O.F. (2002). Hydrate Non-Pipeline Technology, *4th International Conference on Gas Hydrates*, May 19-23., Yokohama, Japan.

Gudmundsson, J.S. (2002). Cold Flow Hydrate Technology, *4th International Conference on Gas Hydrates*, May 19-23., Yokohama, Japan.

Happel, J., Hnatow, M.A. and Meyer, H. (1994). The Study of Separation of Nitrogen from Methane by Hydrate Formation Using a Novel Apparatus, *Annals of the New York Academy of Sciences*, **715**, 412-424.

Herri, J.M., Pic, J.S., Gruy, F. and Cournil, M. (1999). Methane Hydrate Crystallization Mechanism form In-Situ Particle Sizing, *AIChE Journal*, **45**, 3.

Kobayashi, R. and Katz, D.L. (1951). Vapor-Liquid Equilibria for Binary Hydrocarbon-Water Systems, *Industrial Engineering and Chemistry*, **45**, 440-451.

Levik, O.I, Monfort, J.P. and Gudmundsson, J.S. (2002). Effects of the Driving Force on the Composition of Natural Gas Hydrates, *4th International Conference on Gas Hydrates*, May 19-23., Yokohama, Japan.

Monfort, J.P., Jussaume, L., El Hafaia, T. and Canselier, J.P. (2000). Kinetics of Gas Hydrate Formation and Tests of Efficiency of Kinetic Inhibitors, Experimental and

Theoretical Approaches, *Annals of the New York Academy of Sciences*, **912**, 753-765.
Mullin, J.W. (1993). *Crystallization*, 3rd ed., Butterworth-Heinemann Ltd., 209-215.
Oldshue, J.Y. (1983). *Fluid Mixing Technology*, McGraw-Hill Pub. Co.
Parlaktuna M. and Gudmundsson, J.S. (1998a). *Continuous Production Rate of Hydrate, Effect of RPM, Pressure and Gas Injection Rate*, Technical Report, Department of Petroleum Engineering and Applied Geophysics, NTNU.
Parlaktuna M. and Gudmundsson, J.S. (1998b). Continuous Production Rate of Hydrate, *Effect of Sub-cooling and Gas Injection Rate,* Technical Report*,* Department of Petroleum Engineering and Applied Geophysics, NTNU.
Perry, R.H. and Green, D. (1986). *Perry's Chemical Engineers' Handbook*, 6th ed., McGraw-Hill Int. Editions.
Polymath 5.1 (2002). The CACHE Corporation, The University of Connecticut, Ben Gurion University of the Negev and The University of Michigan.
Skovborg, P. and Rasmussen, P. (1994). A Mass Transport Limited Model for the Growth of Methane and Ethane Gas Hydrates, *Chemical Engineering Science*, **42**, 11, 1131-1143.
Song, K.Y., Feneyrou, G., Fleyfel, F., Martin, R., Lievois, J. and Kobayashi, R. (1997). Solubility measurements of methane and ethane in water at and near hydrate conditions, *Fluid Phase Equilibria*, **128**, 249-260.
Tatterson, G.B. (1991). *Fluid mixing and gas dispersion in agitated tanks,* McGraw-Hill, Inc., 37, 491-497.
Vysniauskas, A. and Bishnoi, P.J. (1983). A Kinetic Study of Methane Hydrate Formation, *Chemical Engineering Science*, **38**, 7, 1061-1072.
Vysniauskas, A. and Bishnoi, P.J. (1985). Kinetics of Ethane Hydrate Formation, *Chemical Engineering Science*, **40**, 2, 299-303.